Scintillation Properties and Temperature Responses of $Cs_2LiLaBr_6:Ce^{3+}$

Kan Yang, *Member, IEEE,* Peter R. Menge, *Member, IEEE,*
Julien Lejay, and Vladimir Ouspenski

***Abstract*– This report presents the scintillation properties and temperature dependent neutron and gamma responses of $Cs_2LiLaBr_6$ elpasolite crystals with 0.5, 2, and 3.5% Ce doping. $Cs_2LiLaBr_6$ has excellent scintillation light output proportionality, high light output, and good energy resolution. It also shows good light output temperature stability. Pulse shape differences between neutron and gamma excited pulses are analyzed as a function of temperature. Neutron-gamma pulse shape discrimination is possible in a wide temperature range from -10°C up to at least 140 °C.**

I. INTRODUCTION

CERIUM doped $Cs_2LiLaBr_6:Ce^{3+}$ ($CLLB:Ce^{3+}$) elpasolite crystal has attracted interest as an excellent detector of gamma rays [1,2]. Almost as interesting is its ability to discriminate neutron detections from gamma-rays via pulse shape. Although pulse-shape discrimination (PSD) in CLLB is not as distinct as in fellow elpasolite, Cs_2LiYCl_6 (CLYC), CLLB is superior in light yield and energy resolution. Thus, interest exists in optimizing the gamma ray response and the PSD through changes in dopant concentration and improved PSD techniques.

Whereas CLYC has been shown to lose light output and PSD ability with increasing temperature [3,4], CLLB has gone unexamined with regard to extreme temperature excursions. An additional purpose of this work is to study the suitability of using CLLB as a neutron / gamma detector in low and high temperature applications such as oil well-logging and space flight.

II. EXPERIMENTAL

All CLLB crystals studied in this research were grown by Saint-Gobain Crystals. Table 1 lists the three CLLB samples used in this study. Their photo is shown in Fig. 1. Both 0.5% and 2% Ce doped CLLB crystal are highly transparent and of good quality. The 3.5% Ce doped crystal has cloudy area near its core, which reduces its light output and worsens its energy resolution. We are in the process of improving the crystal quality of CLLB. All crystals were wrapped with Teflon reflector and hermetically packaged in titanium housings with sapphire optical windows on one end. Each crystal was optically coupled to the sapphire window by a clear silicone rubber. This packaging is suitable for a temperature range of -60° to 210° C.

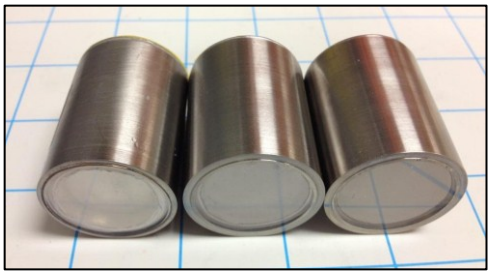

Fig. 1. Photo of CLLB crystals doped with 2%, 0.5% and 3% Ce (from left to right), respectively

TABLE I. $Cs_2LiLaBr_6:Ce^{3+}$ CRYSTALS TESTED

Constituent	Dopant*	Size and Shape
$Cs_2LiLaBr_6$	0.5% Ce^{3+}	Ø1" × 1/4"
$Cs_2LiLaBr_6$	2% Ce^{3+}	Ø1" × 1/2"
$Cs_2LiLaBr_6$	3.5% Ce^{3+}	Ø1" × 1"

*at % in the melt, with respect to La^{3+}

For light output measurements, packaged crystals were coupled to an Electron Tubes 9305KB photomultiplier tube (PMT) with optical grease. Shaping time used is 8 μs. At least 50,000 counts were collected under the full energy peak of a Cs-137 pulse height spectrum to ensure sufficient counting statistics.

For determination of scintillation time profiles, the Time Correlated Single Photon Counting (TCSPC) technique originated by Bollinger and Thomas was used [5]. Two Photonis XP20Y0 PMTs were used for start and stop channels. The stop PMT was located at approximately 50 cm from the sample crystal. An adjustable aperture was used to ensure that the stop PMT only detects single photon events. The stop-to-start count rate ratio was kept below 5% for all measurements. The system was calibrated by an ORTEC 462 time calibrator before the measurements.

UV Emission and excitation spectra were measured with a Varian Eclipse Spectrophotometer. UV light from a Xenon lamp selected by a monochromator was used to excite the crystals. Light emission from the same surface as excitation was then recorded by a PMT through the emission monochromator.

Manuscript received November 16, 2012.

Kan Yang is with Saint-Gobain Crystals, Hiram OH 44234 USA (telephone: 440-834-5697, e-mail: kan.yang@saint-gobain.com).

Peter R. Menge is with Saint-Gobain Crystals, Hiram OH 44234 USA

Julien Lejay and Vladimir Ouspenski is with Saint-Gobain Recherche, 39 Quai Lucien Lefranc 93303 Aubervilliers France.

978-1-4799-0534-8/13/$31.00 ©2013 IEEE

For scintillation light output proportionality, a close-coupled Compton coincidence system was set up based on the design in [6]. The sample was coupled to a Hamamatsu R1306 PMT with optical grease. A ^{65}Zn source (1115.546 keV) was used to excite the crystal. An Ortec GMX-30200-P HPGe detector was used to capture the Compton scattered gamma rays. Coincidence pulses from HPGe and PMT were recorded for a period of 30 minutes. Then un-gated pulses were recorded for both PMT and HPGe for 5 minutes in between data acquisition in coincidence mode. Centroids of un-gated pulse height spectra were continuously tracked to correct for the gain drifting in both detectors.

For temperature dependence measurements of scintillation light output, the packaged crystal was coupled to one end of a quartz light pipe. No optical couplant was used. The other end of the quartz light pipe was coupled to a Photonis XP20Y0 PMT with silicone rubber. The sample end of the quartz light pipe was inserted through a sample port into an environmental chamber. The PMT end of the quartz light pipe was kept outside the environmental chamber throughout the measurement so that the temperature of PMT could be kept at room temperature. The quartz light pipe was wrapped with multiple layers of aluminum foils to enhance light collection efficiency. A 5 μCi ^{137}Cs metal sealed source was placed in the close vicinity of the crystal inside the environmental chamber. Crystals were ramped up to 175^{o} C then down to -40 ^{o}C. A slow ramp rate (6 ^{o}C/hour) was used in order to minimize the thermal lag and eliminate the temperature gradient inside the crystal. A thermocouple was taped directly on the surface of the crystal housing to record its temperature. Pulse height spectra were measured continuously every 5 minutes and Labview-based software was used to record the multi-channel analyzer data (MCA) and automatically track the centroid of full energy peaks.

Pulse shape experiments at varying temperatures used essentially the same set-up as described in the previous paragraph. However, the anode signal of the PMT was connected to a CAEN 5751 digitizer with 1GHz sampling rate for subsequent PSD analysis. A ^{252}Cf source was used to excite the crystal with both gamma and neutron radiation.

III. Results and Discussions

A. Scintillation Properties

Table 2 compares the relative light output of CLLB crystals with 0.5%, 2% and 3.5% Ce doping. CLLB doped with 2% shows the highest light output as well as the best energy resolution among all crystals. Due to the cloudy area in the 3.5% Ce crystal, it shows lower light output and worse energy resolution than the other two. The performance of 3.5% Ce is expected to be improved significantly after crystal growth optimization. Fig 2 compares the pulse height spectra of $LaBr_3$:Ce and CLLB:2%Ce.

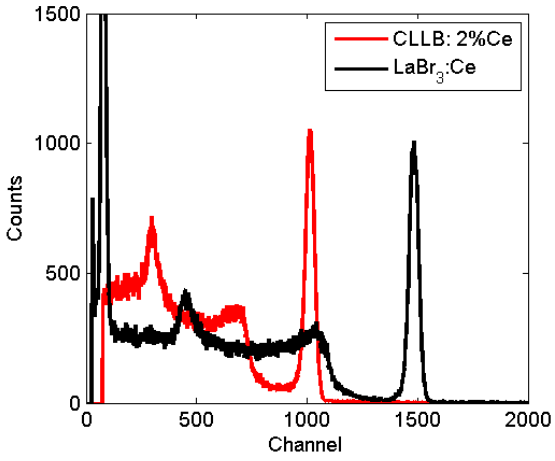

Fig. 2. Pulse height spectra of CLLB:2%Ce and $LaBr_3$:Ce

TABLE II. SCINTILLATION LIGHT OUTPUT OF CLLB

Composition	Relative Light Output (% of $LaBr_3$:Ce)	Energy Resolution[1]
0.5% Ce	56%	7.3%
2% Ce	68%	4.6%
3.5% Ce	39%	8.6%

[1] Measured at 662 keV

The scintillation time profiles of 0.5%, 2% and 3.5% Ce doped CLLB crystals are shown in Fig. 3. All time profiles can be fitted with double-exponential decay models. The decay constants are shown in Table 3. Time profiles of all crystals consist of a fast decay component around 120 ns and a slow decay component of hundreds of nanoseconds. The decay times of 2% and 3.5% CLLB crystals are almost the same, while the 0.5% Ce doped crystal has significantly more light in the slow component.

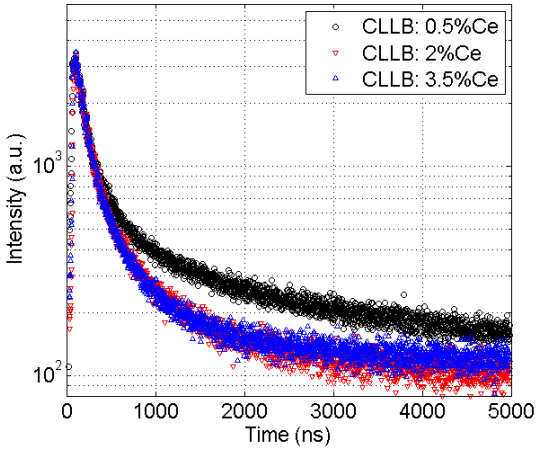

Fig. 3 Scintillation time profiles of 0.5, 2 and 3.5% Ce doped CLLB

TABLE III SCINTILLATION DECAY TIMES OF CLLB

Composition	Decay constants (ns)	
	τ_1	τ_2
0.5% Ce	116 (53%)	975(47%)
2% Ce	122 (61%)	661(39%)
3.5% Ce	125 (64%)	590 (36%)

B. *Emission Characteristics*

Fig. 4 shows UV excited emission and excitation spectra of of 0.5, 2 and 3.5% Ce doped CLLB crystals. Characteristic Ce 4f-5d transitions are observed. The overlap between excitation and emission spectra increases with increasing Ce concentration. The intensity of Ce emission peak at 391 nm also decreases. This indicates some level of self-absorption. The CLLB: 3.5% Ce shows an additional excitation peak at 285 nm. This most likely relates to additional defects introduced by high Ce concentration.

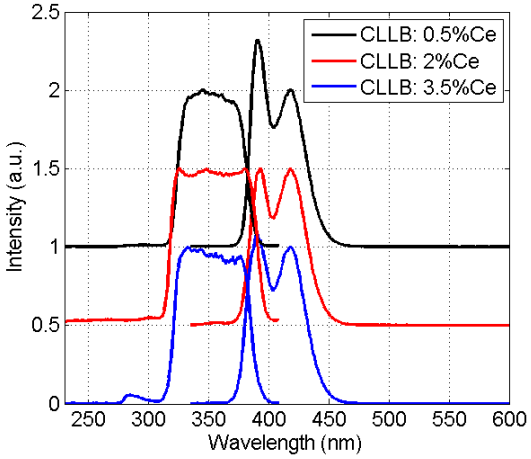

Fig. 4. UV emission and excitation spectra of 0.5, 2 and 3.5% Ce doped CLLB crystals; excitation spectra were measured at 418 nm emission and emission spectra were measured under 325 nm UV excitation.

C. *Proportionality*

Fig. 5 shows the electron response curves of both CLLB:2% Ce and $LaBr_3$:Ce measured by the close coupled Compton coincidence technique. Error bars are not shown for clarity. At any point, fitting error does not exceed ±1%. As we can see in the figure, the electron response proportionality of CLLB is fairly close to ideal response over the range 13 – 600 keV, which agrees with the gamma response proportionality measured by various gamma energies [2]. The proportionality is significantly better than that of $LaBr_3$:Ce. This indicates that there is room for energy resolution improvement for CLLB crystals. The measured energy resolution in Table 2 is by large extent determined by crystal quality, uniformity and the amount light scattering in the crystals. These properties are expected to improve as growth parameters are optimized.

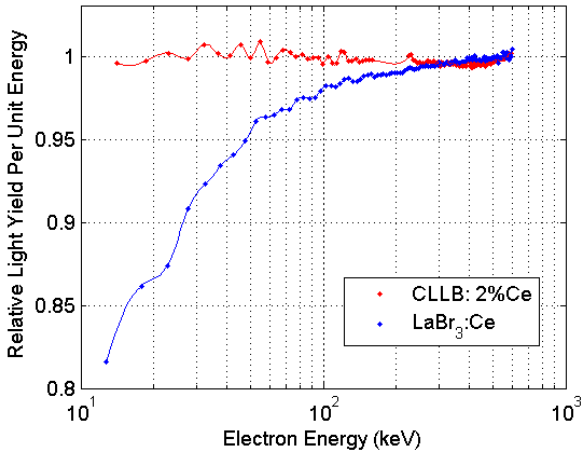

Fig. 5 Electron response curve of CLLB:2%Ce and $LaBr_3$:Ce

E. *Temperature dependence of scintillation light output*

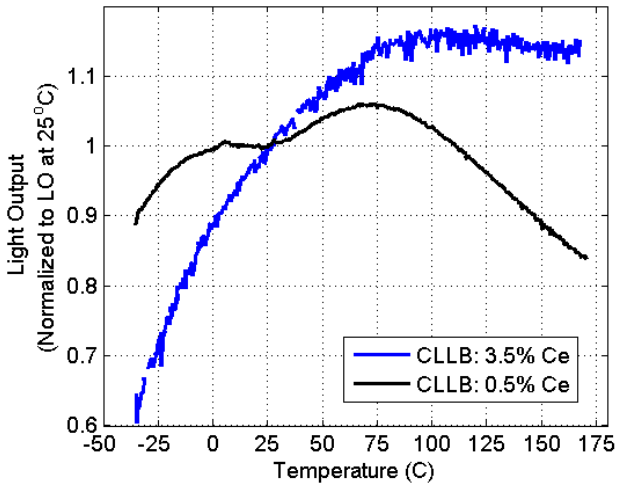

Fig. 6. Scintillation time profiles of 0.5, 2 and 3.5% Ce doped CLLB

The temperature dependence of scintillation light output is presented for CLLB:0.5% Ce and 3.5% Ce. Unfortunately, the 2% Ce doped CLLB sample was damaged before the measurement. Temperature response of the 2% Ce doped CLLB will be included in future reports.

The 3.5% Ce doped CLLB has an interesting temperature response curve. It loses about 40% of its light at room temperature when cooled to ~35 °C. Above room temperature, the light output of CLLB:3.5% Ce crystal increases when temperature increases. From 25 °C to ~100 °C, the light output of CLLB: 3.5% Ce increases by ~15%. Then the light output remains stable in the temperature range between 100 °C and ~175 °C.

The 0.5% Ce doped CLLB behaves a little differently than the 3.5% Ce doped CLLB. It loses less light output when cooled, but it loses more when heated to ~175 °C (about -15%).

F. *Pulse shape discrimination*

Fig. 7 shows the averaged pulses for both gamma and neutron excited pulses in CLLB: 2%Ce. Unlike CLYC [7-9], core-valence luminescence is not present in CLLB. Neutron excited pulses are found to be faster than gamma excited pulses in both rise and decay. This is believed to be caused by a bi-molecular decay process where the shape of the decay curve depends on the initial excitation density [9,10].

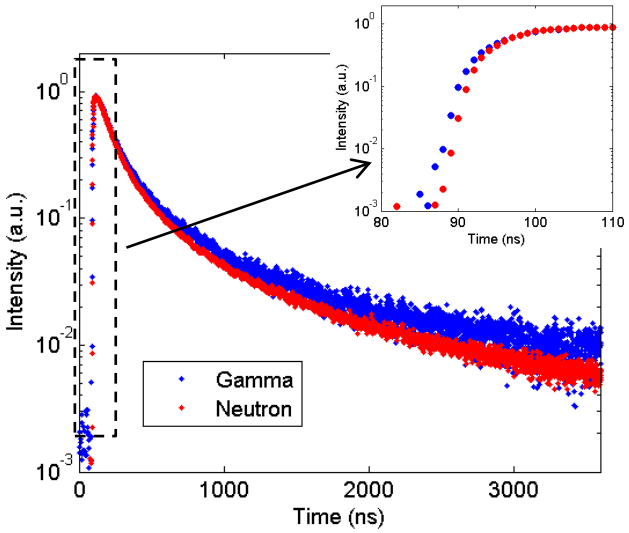

Fig. 7 Averaged gamma and neutron pulses for CLLB:2%Ce

Using a pre-determined sorting algorithm, a pulse descriptor or PSD parameter can be generated for each single pulse. Fig. 8 shows an example PSD scatter plot generated by using the PSD parameter as y-axis and pulse height as x-axis. The pulses from neutron capture reaction on ^{6}Li clearly distinguish themselves from the gamma excited pulses. In order to quantitatively compare the performance of PSD algorithms, a LLD is set at 3 MeV to reject any pulses with lower pulse height. A histogram of PSD parameters (right plot in Fig. 8) is generated for all pulses above the threshold. A PSD Figure of Merit (FOM) is defined by the equation below.

$$FOM = \frac{H_1 - H_2}{FWHM_1 + FWHM_2}$$

Where H_1 and H_2 are centroids of the Gaussian fitted peaks and $FWHM_1$ and $FWHM_2$ are the full-width-half-maximum of each Gaussian fitting.

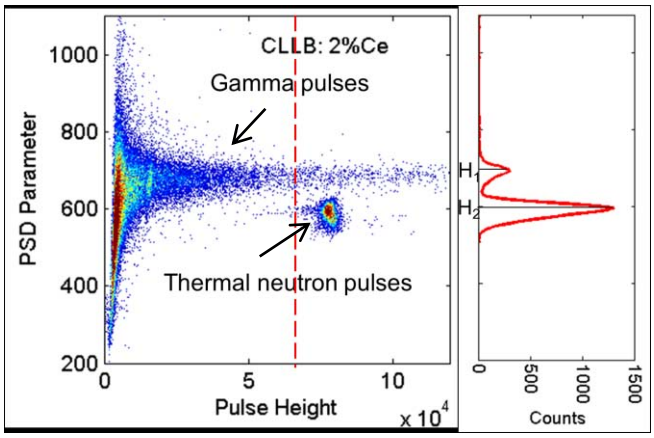

Fig. 8 PSD scatter plot of CLLB:2%Ce excited with Cf-252 (left); histogram of PSD parameter (right)

The relative difference in the rise part of the pulse is more prominent than the difference in the decay part in terms of integrated intensity. In order to optimize the performance of PSD, the sorting algorithm should allocate more weight to the rise part. Table 4 compares the PSD FOM derived from several example PSD algorithms. The same data set recorded from the CLLB:2%Ce sample is used.

For the charge comparison method, the PSD parameter for each pulse is derived from the ratio of two integration time windows. Usually one includes the first 100 ~500 ns of the pulse and the other window includes the following several µs. For the 10-90% rise time algorithm, the PSD parameter is derived from the time for the pulse integral to rise from 10% to 90% of this final value. The same definition applies to the 2-60% rise time algorithm. The PSD parameter can also be derived from the Fourier transform of each pulse based on the percentage of the principal component. The 2-60% rise time algorithm is found to yield the highest FOM because it puts more weight on the rise part on the pulse..

TABLE IV COMPARISON OF EXAMPLE PSD ALGORITHMS FOR CLLB: 2%CE

PSD Algorithm	FOM
Charge Comparison	1.22
Fourier Transform	1.26
10-90% rise time	1.00
2-60% rise time	1.34

The same analyses were also performed for 0.5 and 3.5% Ce doped CLLB crystals. Due to the cloudiness in the core, the 3.5% Ce does not yield satisfactory PSD resolution. Table 5 lists the PSD performance of different CLLB samples. The 2% Ce doped CLLB crystal shows the best PSD performance.

TABLE V PSD PERFORMANCE OF DIFFERENT CLLB SAMPLES

Composition	GEE (MeV)	FOM
0.5% Ce	3.27	1.02
2% Ce	3.27	1.34
3.5% Ce	3.3 ± 0.3	/

G. *Temperature dependence of PSD characteristics*

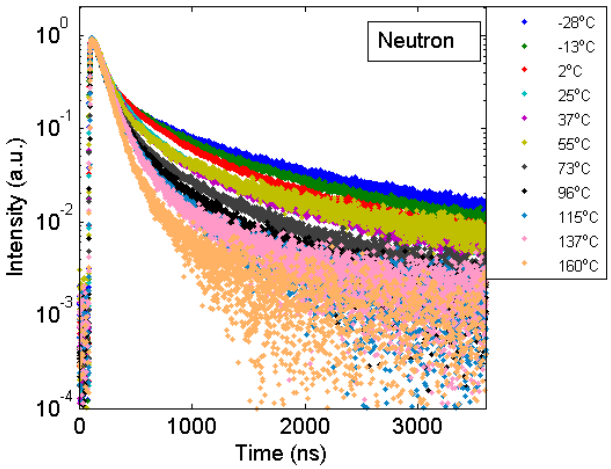

Fig. 9 Neutron excited pulses of CLLB: 2%Ce at different temperatures

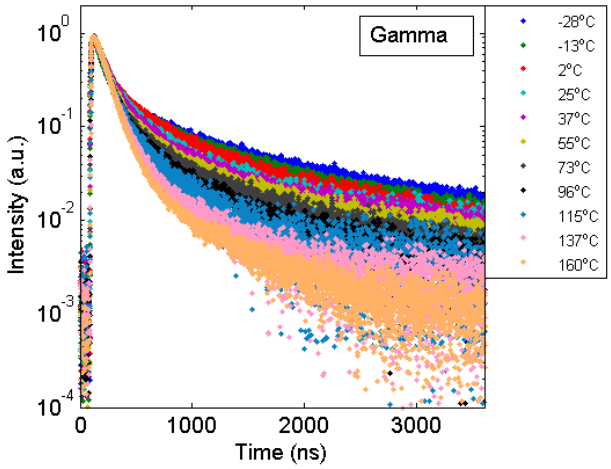

Fig.10 Gamma excited pulses of CLLB: 2%Ce at different temperatures

The PSD characteristics of CLLB:2%Ce are studied at different temperatures. Figs. 9 and 10 illustrate the shape of neutron or gamma excited scintillation pulses as a function of temperature. For either neutron or gamma excited pulses, the scintillation time profiles are expedited with increasing temperature. In other words, the fast decay components become more prominent with increasing temperature. It is worth noting that the fast components of both neutron and gamma excited pulses are almost completely suppressed when the crystals are cooled down to -28 ^{o}C.

By applying the same PSD algorithm described in the previous section, we can plot the histograms of PSD parameter at different temperatures. Fig. 11 and 12 shows the PSD histograms at different temperatures and their corresponding PSD FOM.

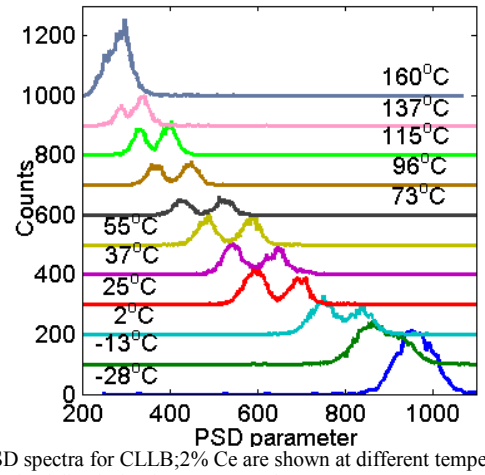

Fig. 11 PSD spectra for CLLB;2% Ce are shown at different temperatures. Note the lack of discrimination at -28° and +160° C

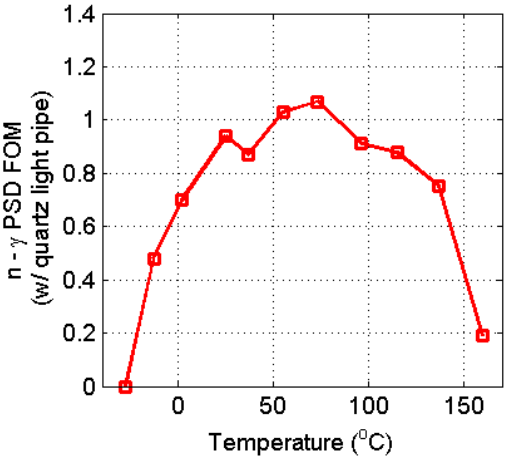

Fig. 12. The PSD FoMfor CLLB:2% Ce is shown as a function of temperature.

Interestingly, when the CLLB crystal is cooled down to -28 ^{o}C, pulse shape differences between gamma and neutron diminish. The gamma and neutron peak on the PSD histogram merge into one and become indistinguishable. However, the crystal retains its PSD capability in a wide temperature range from -13^{o}C to at least ~140^{o}C, which enables the possibility for down-hole gamma and neutron measurements in oil well logging applications.

IV. Summary

Both 0.5% and 3.5% Ce doped CLLB crystals show good light output temperature stability. Neutron excited pulses are found to be faster than gamma excited pulses in both rise and decay. Neutron-gamma PSD in CLLB is preserved in a wide temperature range from RT up to at least 140 ^{o}C. Future work will focus on optimizing the crystal quality and further improving the neutron-gamma responses via co-doping.

References

[1] J. Glodo, et al., IEEE TNS, 58:333-338, 2011.
[2] U. Shirwadkar, et al., NIMA, 652:268-270, 2011.
[3] Menge, P.R., et. al., *Nuclear Science Symposium and Medical Imaging Conference (NSS/MIC), 2011 IEEE* , pp.1598-1601, 23-29 Oct. 2011
[4] Budden, B.S., et. al., *IEEE Trans. Nuc. Sci.* , vol.60, no.2, pp.946-951, April 2013

[5] L. M. Bollinger, G. E. Thomas, Rev. Sci. Inst. vol.32, no.9, pp.1044-1050, 1961
[6] P.B. Ugorowski et al., NIMA 615, 2, pp.182-187, 2010
[7] J. Glodo et al., IEEE TNS, VOL. 56, NO. 3, JUNE 2009
[8] W.M. Higgins et al. J.of Crystal Growth 312 (2010) 1216–1220
[9] J. Glodo et al., IEEE TNS, vol.59, no.5, pp.2328,2333, Oct. 2012
[10] N. F. Mott and R. W. Gurney, Electronic Processes in Ionic Crystals. Oxford, U.K.: Clarendon, 1948.